Disruption mitigation by massive gas injection at TEXTOR

Bozhenkov S. A.[1], Finken K. H.[1], Lehnen M.[1], Wolf R. C.[2], Jakubowski M. W.[2],
Liang Y.[1], Uzgel E.[1], Van Wassenhove G.[3], Zimmerman O.[1] and the TEXTOR team
[1] *Institute for Energy Research - Plasma Physics, Forschungzentrum Jülich GmbH, EURATOM-Association, Trilateral Euregio Cluster, D-52425 Juelich, Germany*
[2] *Max-Planck-Institut für Plasmaphysik, D-17491 Greifswald, Germany*
[3] *Laboratoire de Physique des Plasmas/Laboratorium voor Plasmafysica, ERM/KMS, EURATOM Association, B-1000 Brussels, Belgium*

Disruptions represent a threat for fusion experiments and reactors to come. Associated heat fluxes can lead to significant wall erosion. In elongated plasmas loss of the vertical control leads to excitation of halo currents. Since they are closed in the wall, the vessel is subjected to strong $\vec{j} \times \vec{B}$ forces. Moreover, the induced electric field appearing in the cold plasma is able to accelerate runaway electrons, whose total energy can reach in ITER 1 GJ. Mitigation techniques considered in the community are “killer” pellet and massive gas injection (MGI). Pellets reduce heat loads by up to 90% by radiatively redistributing heat fluxes and diminish halo currents by 50% by making the current decay faster. But the resulting electron density turns out to be insufficient to unconditionally suppress runaway electrons (RE). Massive injection of noble gases (more than ten times the number of atoms achieved by a pellet) also softens heat fluxes and EM forces. However understanding of the underlying mechanisms remains poor: only recently the shutdown was recognized to be disruptive, with flux surface $q = 2$ being critical for the onset of the thermal quench (TQ) [1].

Here we report on MGI experiments performed at TEXTOR (major and minor radii are 1.75 m and 0.46 m) into stable discharges with the following parameters: toroidal field $B_t = 2.25$ T, plasma current $I_p = 350$ kA (magnetic energy $E_{mag} \approx 300$ kJ), line averaged electron density $< n_e >= 2 \cdot 10^{19}$ m $^{-3}$, thermal energy content $E_{th} \approx 40$ kJ. Gas was injected by a fast valve driven by eddy currents. It combines fast reaction time with the immunity against high static magnetic fields and provides flow rates in the range $(20 \div 8500) \cdot 10^{22}$ particles·s^{-1} and total amount of atoms $(0.16 - 5) \cdot 10^{22}$ [2]. The upper boundary on the gas amount indicated here is limited only by the TEXTOR vacuum system. Gases used in the experiments include deuterium, helium, argon and mixtures of argon and deuterium containing 5, 10 and 20% of argon.

The MGI shutdown consists of four main stages: 1 - sonic gas flow in the vacuum duct; 2 - predisruptive phase characterized by cooling of the edge regions; 3 - thermal quench (TQ); 4 - current quench (CQ) [3]. In the predisruptive phase the cold front penetrates only to the $q = 2$ flux surface as observed by the 2nd harmonics of ECE, Thomson scattering and fast camera. An example of Thomson scattering data is presented in figure 1 for an injection of $2.1 \cdot 10^{22}$ atoms

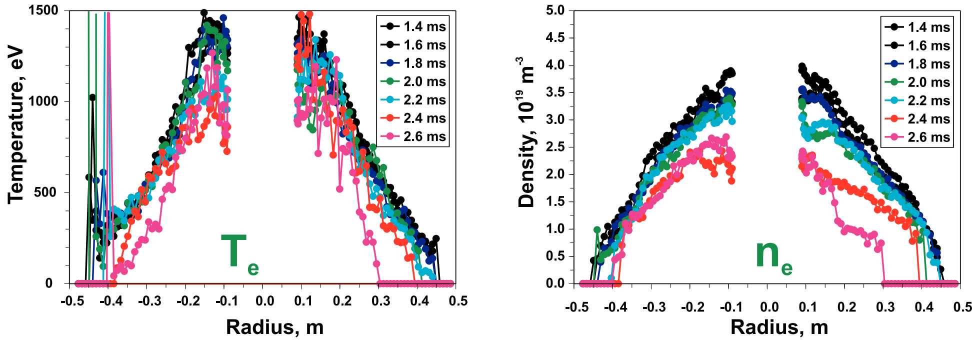

Figure 1: Thomson scattering measurements. #102526, MGI $2.1 \cdot 10^{22}$ atoms of Ar. Gas arrived to the plasma edge at $t_G = 1.6$ ms, TQ started at $t_{TQ} \approx 2.7$ ms (drop of central temperature by 20%). Time is given relative to the trigger of the valve.

of argon. One observes a distinct edge cooling and at the same time preservation of the core temperature and about a drop of the central density by 30%. Note that in the TQ phase Thomson scattering measurements are not reliable because of the plasma background light dominating the laser signal. The position of the emission front observed in different spectral lines is illustrated in figure 2. The gas is injected from the top of the torus, the position of the inner wall (HFS) is outlined by the cyan points, while the green ones mark the $q = 2$ surface in the plane parallel to the lens. The location of the emission front around $q = 2$ was confirmed by a qualitative similarity of the images recorded in the experiment (fig.2) with those simulated under the assumption of optically thin plasma for the δ-like radial distribution of the emissivity. That is, we estimated the integral $\int \Omega d^3V$ over the volume imaged to a particular pixel, where Ω is the solid angle based on the lens diameter. In addition, a simple comparison of the energy lost by the plasma before the TQ with that consumed by ionization, heating and radiation of the gas indicates that the position of the emission front has to coincide with the location of the injected particles. The last fact can also be concluded from density measurements with Thomson scattering.

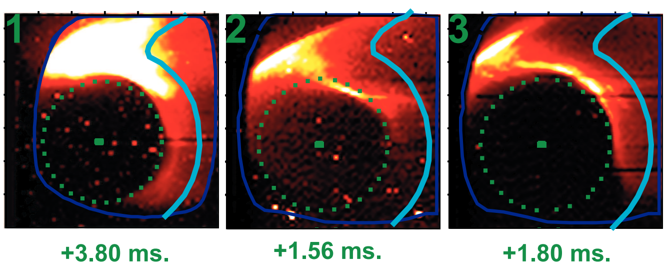

Figure 2: Emission front at onset of TQ. 1 - #100165, MGI $0.31 \cdot 10^{22}$ atoms of Ar, ArII 442 light. TQ started at $t_{TQ} \approx 4.1$ ms. 2 - #102518, MGI $2.6 \cdot 10^{22}$ atoms of He, HeII 468 light. $t_{TQ} \approx 1.6$ ms. 3 -#102520, MGI $1.5 \cdot 10^{22}$ atoms of Ar10%+$D_2$90%, ArII 611 light. $t_{TQ} \approx 2.0$ ms. Cyan points outline the inner wall. Green points mark the $q = 2$ surface in the plane parallel to the lens.

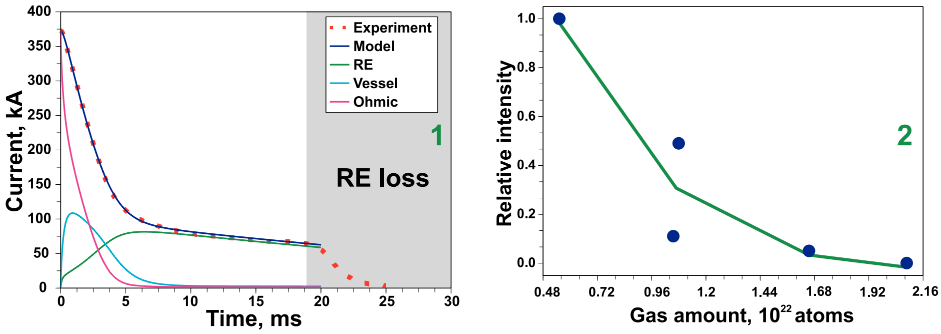

Figure 3: 1 - Modeled and measured currents, #102521, injection of $0.5 \cdot 10^{22}$ atoms of Ar. 2 - peak synchrotron emission for a number of argon shots. The green line is to guide the eye only.

The further development of a MGI discharge demonstrates bursts of X-ray emission, of MHD fluctuations (dB_p/dt) and of the limiter potential. The X-ray emission mentioned here is seen by the fast camera as a noise pattern and by the SXR camera as an intensity increase simultaneous on all chords. After this phase, the SXR intensity drops in 0.5 ms for mixtures containing Ar and in about 1 ms for He over the whole plasma center without distinct cold front. It is this last stage that is usually called thermal quench. In low pressure ($N < 0.35 \cdot 10^{22}$ atoms) injections of pure deuterium or helium, the TQ has in fact two steps, with a "silent" phase lasting $1 \div 2$ ms, which is likely to be explained by their low cooling capability. The disruptive nature of MGI is also confirmed by the positive current peak before the CQ, which is known to be a disruption feature related to a flattening of the current density profile. These results are in correspondence with recent data from DIII-D [1].

In the CQ phase the current decays at rates that in general depend on the type and amount of injected gas. The slowest decay of about 70 MA$\cdot$s^{-1} and a very weak dependence on the amount of atoms are typical for helium, while shots terminated by mixtures containing argon show faster decay rates and increasing trend towards larger number of atoms $70 \div 120$ MA$\cdot$s^{-1} for $N = (0.2 \div 1.9) \cdot 10^{22}$ atoms. Since measurements of the current are performed outside of the vessel, the given values have to be corrected for currents induced in the vessel. A simple analysis based on two lumped circuits indicates that the values for argon mixtures might be about two times higher, while for the helium case they are almost unaffected. The achieved acceleration of the current quench phase is advantageous for the reduction of halo currents. Diagnostics for direct measurements of halo currents is currently not in operation at TEXTOR.

Injections of pure argon provoke generation of runaway electrons carrying up to 30% of the initial current (fig. 3). The RE population contains a considerable high energy tail ($\varepsilon > 10$ MeV) since its synchrotron emission is visible in the near IR range ($\lambda = 3 \div 5$ μm) and strong neutron/γ fluxes are registered. Increasing the number of injected atoms reduces density of both low and high energy runaways as illustrated by the decrease of the synchrotron emission (fig. 3). To understand reasons for RE appearance a simple 0D model was implemented. The model consists of equations for plasma current including both ohmic I_Ω and runaway I_{RE} parts, vessel current I_v, generation of RE (including primary $f_{primary}$ and secondary mechanisms γ_{RE}) and evolution of T_e in coronal equilibrium:

$$\frac{dn_{RE}}{dt} = f_{primary}(E, n_e, T_e) + (\gamma_{RE}(E, n_e) - \gamma_{loss})n_{RE}$$

$$\frac{d}{dt}\left(LI_\Omega + L_{RE}I_{RE} + L_v I_v\right) = -2\pi R_0 E_{ind}$$

$$\frac{d}{dt}\left(I_v + I_\Omega + I_{RE}\right) = -\frac{I_v}{\tau_v}$$

$$\frac{d}{dt}\left(n_e T_e\right) = \frac{2}{3}\left(\eta\frac{I_\Omega^2}{S^2} - n_{atoms}n_e \cdot L_{rad}(T_e) - n_e n_i \gamma_{ei}(T_e - T_i)\right)$$

$$\frac{d}{dt}\left(n_i T_i\right) = \frac{2}{3} n_e n_i \gamma_{ei}(T_e - T_i)$$

By varying few free parameters, among which the most critical ones are density of deuterium n_D and of injected atoms n_{atoms}, it is possible to reach a good agreement of modeled current with that measured experimentally (fig. 3). The necessary condition for RE proved to be low central argon density. To be precise, the found density n_{atoms} constitutes not more than 3% of that to be expected for the uniform distribution of atoms, with the sensitivity analysis indicating the uncertainty not more than a factor of 2 or 3. Similar modeling of argon mixture and pure helium results in mixing efficiencies of about 20% and 40% correspondingly. But the absence of RE is explained not by lowering the induced field below the critical one but rather by the inefficiency of the primary mechanism (small E_{ind}/E_D) and small secondary multiplication ~ 5.

TEXTOR data indicate that the MGI shutdown is disruptive. The plasma is destabilized when the cold gas reaches the $q = 2$ surface. Mixing of impurities in TQ does provide acceleration of the current decay, which is advantageous for reduction of halo currents. However in low pressure argon injections ($N < 1.2 \cdot 10^{22}$ atoms) the resulting electron density is not enough to suppress RE. If the RE beam is present it contains a considerable amount of particles with energies above 10 MeV. The fact that REs are not generated in experiments with larger amounts of argon or with other gasses is to be attributed to the suppression of the primary mechanism and low secondary multiplication.

References

[1] Hollmann E. M., Jernigan T. C., et al., Phys. Plasmas, 14 (2007), p. 012502

[2] Bozhenkov S.A., Finken K.-H., Rev. of Sci. Instrum., vol. 78 (2007), p. 033503

[3] Bozhenkov S.A., Finken K.-H., et al., 33rd EPS on Plasma Physics, Rome 2006, http://eps2006.frascati.enea.it/papers/pdf/P2_162.pdf